JCTC Journal of Chemical Theory and Computation

Article

pubs.acs.org/JCTC

Multisite Ion Models That Improve Coordination and Free Energy Calculations in Molecular Dynamics Simulations

Akansha Saxena[†,‡] and David Sept*[,†]

[†]Department of Biomedical Engineering and Center for Computational Medicine and Bioinformatics, University of Michigan, Ann Arbor, Michigan 48109, United States

[‡]Department of Physics, Applied Physics and Astronomy, Rensselaer Polytechnic Institute, Troy, New York 12180, United States

Supporting Information

ABSTRACT: Current ion models in molecular mechanics are simple spheres, and their interactions are solely determined from the van der Waals radius of the sphere and the total charge. Here, we introduce a model where we distribute the total charge of the ion into *n*-dummy centers that are placed in the direction of the coordinating atoms. We have parametrized this model for two divalent cations, Ca^{2+} and Mg^{2+}, and have tested the model's accuracy in a variety of simulations. With this model we are not only able to correctly predict the free energies and selectivity for cation binding sites in proteins and nucleic acids, but we achieve better coordination geometries and can capture more subtle effects such as the exchange of inner shell waters. Additionally, this model does not employ higher-order electrostatics and thus can be easily used with standard force fields.

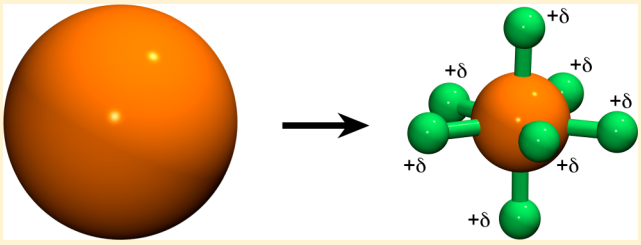

INTRODUCTION

Ions play a significant role in physiology and biochemistry, and their interaction with ion channels, proteins, and nucleic acids are vital for normal biological function. One of the fundamental features of this interaction is *selectivity*, or the binding of a specific ion based on its size, charge and/or coordination geometry. Quantum mechanics calculations allow one to account for selectivity and capture the potentially subtle differences between ions, but standard molecular mechanics potentials have largely been unable to describe these effects since ions are modeled as simple charged spheres. This simplicity is indeed a significant strength of the molecular mechanics approach since it allows the simulation of large, atomically detailed systems, and these simulations give physical insight into the dynamics, kinetics, and thermodynamics of biomolecules. In the case of ions, there are only three basic parameters for a given ion: the charge, and the two parameters describing the Lennard-Jones potential. The charge is fixed to the true value for the ion (i.e., +2 for calcium or magnesium) and the Lennard-Jones parameters are chosen so that the correct hydration free energy is reproduced. However, when one starts to look at the details of ion simulations, several problems are known anecdotally in the field. First, although the hydration free energy can be accurately matched, the solvent structure around the ion is not correct and the inner shell waters are often held too tightly so as to eliminate exchange with the bulk solvent. Second, the thermodynamic predictions for ion interactions with biomolecules are largely incorrect, and the affinity of ion-protein binding or selectivity of a binding site for a specific ion cannot be reproduced. Finally, the interaction of divalent cations with nucleic acids is nearly impossible to capture using molecular mechanics, independent of the force field selected.

In order to solve these shortcomings, there has been extensive work in simulation and (re)parametrization of the force field parameters for many different ions.[1−10] Further, with the development of polarizable force fields, it has become possible to account for the many-body terms by the use of the polarization term,[11−14] although these simulations extract a larger computational cost. One particularly interesting approach is to distribute the charge and van der Waals centers to multiple sites. This has been done in past work for manganese,[15] zinc,[16−18] and magnesium.[19] In this work, we present comparable models for calcium and magnesium. Inspired by Pauling's electrostatic valency principle,[20] we replace the single sphere with a central atom connected to multiple "dummy" atoms along the lines of coordinating bonds (Figure 1). This significantly increases the degrees of freedom, since there are now many possibilities for distributing the electrostatic and steric interaction points; however, through multiple trials we determined that the optimal choice appears to be restricting the bulk of the steric interactions to the central atom while distributing all of the charge to the dummy atoms leaving the central atom uncharged. This choice is easily justified since this keeps the steric interactions centrosymmetric and moving all the charge to the dummy atoms is the truest manifestation of the electrostatic valency principle.

Received: March 6, 2013
Published: July 3, 2013

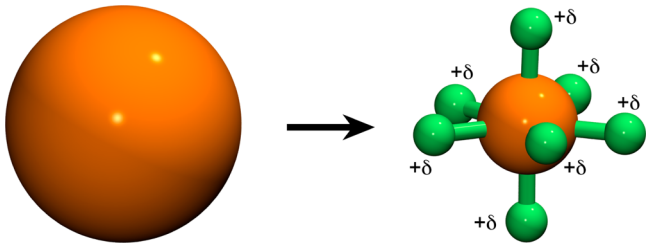

Figure 1. Illustration of our multisite ion model for calcium. Instead of a simple sphere, the charge centers are now distributed to multiple sites depending on the coordination geometry of the ion.

COMPUTATIONAL METHODS

Quantum Calculations on Ion−Water Complexes. From coordination chemistry, it is known that Ca^{2+} can have 6 to 8 coordinating atoms; however, the most common geometry observed in biological systems is pentagonal bipyramid geometry.[21] Mg^{2+} has a smaller radius and has a strict octahedral coordination geometry.[22] Inspired by these studies, the multisite cation model for Ca^{2+} was started with a pentagonal bipyramid geometry with $n = 7$ and for Mg^{2+} an octahedral geometry with $n = 6$. Complexes of the cations, $[Ca(H_2O)_7]^{2+}$ with the first solvation shell and $[Mg(H_2O)_6]^{2+}(H_2O)_{12}$ with the first and second solvation shells were minimized with quantum mechanical calculations using GAUSSIAN.[23] Since the second solvation shell for Ca^{2+} lacks a well-defined geometry, it was not included. The calculations were divided into two steps: first, a geometry optimization was performed to get the optimized structure of the complex, and then, the single point energy was evaluated. B3LYP method and 6-311+G(2d,2p) basis set were used for both steps. 6-311+G(2d,2p) basis set has two sets of polarization functions on all atoms and diffuse functions, which are important for interactions with oxygen in water containing systems. A smaller basis set LANL2DZ was also tried for optimizations but the former gave better energies.

The optimized structure of the Ca^{2+} complex showed a regular pentagonal bipyramid geometry with Ca−O distances of 2.4 Å. This structure matched with the one obtained from *ab initio* molecular orbital calculations in other works.[24] The final Mg^{2+} complex showed an octagonal geometry for the first solvation shell with 6 water molecules and distances of 2.1 Å for Mg−O. The second solvation shell consisted of 12 water molecules hydrogen bonded to the inner-shell water molecules. The geometry of this complex could be represented as a pentagonal dodecahedron arrangement of water molecules enclosing the $[Mg(H_2O)_6]^{2+}$ octahedron, and it matched very well with results obtained from molecular orbital theory and density functional theory.[25]

Bond and Angle Terms. Based on the optimized structures of the ion and their first solvation shells, we placed dummy atoms along the vectors connecting the ion center and the coordinating oxygens. We want the dummy atoms to be inside the van der Waals radius of the central atom and following a previous model[17] we selected an equilibrium length of 0.9 Å, a bond stretching force constant of 540 kcal/mol·Å^2, and an angle bending force constant of 55 kcal/mol·radian^2. The equilibrium angles for the case of magnesium are all 90 or 180°, while for calcium the various pairs have angles of 72, 90, 144, or 180°.

Nonbonded Terms. The nonbonded interactions of the cation involve two contributions: electrostatics via the partial charges on the central and dummy atoms and van der Waals interactions using the Lennard-Jones potential. Each dummy atom was assumed to have the same atom type and thus carry identical charge and have the same Lennard-Jones parameters. As detailed in the main text, we considered Pauling's "electrostatic valency principle" and distributed the entire charge of the ion to the dummy atoms, leaving the charge on the central atom zero. This choice differs from previous models,[19] but based on test simulations using different charge distributions, we find this choice is critical for many aspects of our model, particularly the free energy calculations and differentiation of calcium and magnesium (simulation parameters available as Supporting Information). The Lennard-Jones parameters were found from matching hydration free energies as discussed in the main text.

Ion−Solvent Simulations. Each multisite cation model, Ca^{2+} and Mg^{2+} was used to run a simulation in water. For these simulations, the cation was first solvated in a truncated octahedral periodic boundary cell with 24 Å TIP3P water padding. A 10 Å direct-space cutoff was used for short-range Lennard-Jones and electrostatic interactions, long-range electrostatics were treated by Particle Mesh Ewald method (PME), and the covalent bonds to hydrogen atoms were constrained with SHAKE. The system was first minimized by using a hybrid method of switching between steepest descent and conjugate gradient method after every 10 steps and then equilibrated to 298 K, heating gradually in 50 K/10 ps steps for 200 ps. These were followed by the production phase of the system in an NPT ensemble for 50 ns. All calculations used 1 fs time step in the equilibration phases and 2 fs time step in the production phase. The temperature control in all simulations was performed by Langevin dynamics with a collision frequency of 3 ps^{-1}. These and all other simulations were performed using AMBER.[26]

Ion−Protein Simulations. To test the thermodynamics of our multisite ion model in a protein system, we looked at the relative binding energy, $\Delta\Delta G$, of Ca^{2+} vs Mg^{2+} to Site II of Calbindin. The Ca^{2+} bound structure of calbindin (3ICB[27]) and the Mg^{2+}-bound structure (1IG5[28]) were each used, and we ran two sets of simulations: one using a spherical ion model and the other using the multisite cation model with identical simulation conditions. The starting structure was first solvated in a truncated octahedral periodic boundary cell with 12 Å TIP3P water padding. Na^+ and Cl^- counterions were used at a salt concentration of 50 mM. A 10 Å direct space cutoff was used for short-range Lennard-Jones and electrostatic interactions. Long-range electrostatics was treated by Particle Mesh Ewald method (PME), and the covalent bonds to hydrogen atoms were constrained with SHAKE. The system was first minimized by using a hybrid method of switching between steepest descent and conjugate gradient method after every 10 steps and then equilibrated to 298 K, heating gradually in 50 K/10 ps steps for 200 ps. The equilibration step was divided into two steps: the initial step involved 10 kcal/mol restraints on all protein atoms to keep them from moving away from their starting positions and letting the water box equilibrate for 200 ps. The second step involved NVE simulation without any restraints on any atom for 200 ps. These were followed by the production phase of the system in an NPT ensemble for 80 ns. A time step of 1 fs was used for the equilibration phases, and 2 fs was used for the production run. The temperature control in all simulations was performed by Langevin dynamics with a collision frequency of 3 ps^{-1}.

We performed thermodynamic integration in both directions, transitioning from Ca^{2+} ($\lambda = 0$) to Mg^{2+} ($\lambda = 1$) and vice versa. (23 λ values = 0, 0.0001, 0.01, 0.025, 0.05, 0.075, 0.1, 0.125, 0.15, 0.175, 0.2, 0.225, 0.25, 0.275, 0.3, 0.4, 0.5, 0.6, 0.7, 0.8, 0.9, 0.9999, 1) For every λ value, we first equilibrated for 200 ps, and the change in $\partial U/\partial\lambda$ was averaged over another 200 ps of simulation time. The change in free energy between the two end states was calculated by numerically integrating over all λ. Each set of simulation was done three times, and the mean energy change from these was recorded as the final value.

Ion-RNA Simulations. To test out multisite ion models with nucleic acids, we chose the same bidentate RNA clamp as that used by Petrov.[29] The starting coordinates of the RNA bidentate clamp were extracted from the crystal structure of Hepatitis delta virus Ribozyme, 1CX0,[30] consisting of three bases and two phosphate groups coordinating the ion. The force field used for RNA was AMBER/parm99BSC0 (parm99 with refinement for nucleic acid simulations[31]). The thermodynamic integration was performed just as for the protein case using the identical equilibration and sampling times. As before, we performed simulations in both directions (calcium to magnesium and magnesium to calcium) for both the multisite and spherical ion models.

MODEL PARAMETERIZATION

To parametrize the terms for the Lennard-Jones potential, we used thermodynamic integration to calculate the hydration free energy of each cation. For our multisite ion, the Lennard-Jones potential has the form

$$U_{LJ} = \frac{A_c A_a}{r^{12}} - \frac{B_c B_a}{r^6} + \sum_d \frac{A_d A_a}{r^{12}}$$

where A_a and B_a represent are the terms for an arbitrary atom interacting with our multisite ion, A_c and B_c are the terms for the central atom, and A_d is a repulsive term summed over all dummy atoms. Although our dummy atoms are within the van der Waals radius of the central atom, we still assign them a small repulsive term ($A_d = 0.05$) to keep coordinating atoms from getting too close. The remaining A_c and B_c terms were determined by matching the hydration free energies for each atom. We chose the Noyes et al. values of $\Delta G_{hyd}(Ca^{2+}) = -379.46$ kcal/mol and $\Delta G_{hyd}(Mg^{2+}) = -454.2$ kcal/mol.[32] There has been discussion on the selection of the observed value of solvation free energy,[11,12] most importantly whether experiments or simulations calculate *real* or *intrinsic* hydration free energies, which differ by a constant phase potential.[12] Since our simulations use Ewald summation and thus lack the interphase potential contribution,[33] we added the contribution appropriate for a divalent cation in TIP3P water.[12] The hydration free energy of the ion was obtained by disappearing the ion in a large box of water through thermodynamic integration steps of λ going from 0 to 1 (14 λ values = 0, 0.00922, 0.04794, 0.11505, 0.20634, 0.31608, 0.43738, 0.56262, 0.68392, 0.79366, 0.88495, 0.95206, 0.99078, 1). The equilibration and production runs for these calculations are the same as mentioned in the Methods section for other systems. Also, the use of large water box ensures that the charge screening is accurately implemented. The final nonbonded parameters were obtained by varying both A_c and B_c parameters until the hydration free energy was matched. We tried to keep the overall shape of the ion-oxygen Lennard-Jones potential close to that for Åqvist's parameters.[2] This gave us the upper and lower bounds for variation of A_c and B_c. Table 1 shows the resulting set of parameters for each ion. The performance of the multisite model was compared with the spherical ion models from Åqvist.[2] The nonbonded parameters for the spherical Ca^{2+} and Mg^{2+} models were 264.1, 18.82 (*A*,*B*) and 37, 8.32 (*A*,*B*) respectively. These models were parametrized in a similar way, by matching the calculated hydration free energy of ions to the observed value.

Table 1. Lennard-Jones and Charge Parameters for the Multisite Models of Calcium and Magnesium

ion	A_c	B_c	A_d	q_d
Ca^{2+}	233.2	35.5	0.05	0.2857
Mg^{2+}	27.0	16.7	0.05	0.333

RESULTS

Having parametrized our cation models, our first test was to look at the behavior of these ions in water. In the case of magnesium, the inner shell waters remained intact over the course of 100 ns of simulation time, consistent with slow exchange rate (on the order of microseconds) found in experiments.[34,35] For calcium, the inner solvation shell was much more dynamic, and we observed a mean residence time of about 20 ps, consistent with limits found in previous experimental and computational work.[36,37] The radial distribution functions for each ion also showed excellent agreement with experiments[38−40] (Figure 2) and our multisite model exhibited a well-defined peak corresponding to the second solvation shell.[41] Simulations by others and us[42−44] have had some difficulty in reproducing this second peak using a simple spherical ion model although polarizable force fields can achieve this.[11,13]

Our next test was to look at ion-protein interactions using our multisite models. Canonical Mg^{2+} binding sites (e.g., CheY) typically include multiple coordinating waters and show limited, if any, selectivity for magnesium over calcium. On the other hand, the EF hand motif is highly selective for Ca^{2+} and proteins such as calbindin have been well studied both experimentally and computationally. Figure 3 shows the simulation structure for the two EF hand motifs of calbindin where the calcium in the crystal structure was replaced with our multisite model. Previous simulations of this calbindin structure using a spherical ion model were met with problems since local ion coordination and protein secondary structure were lost;[45,46] however, most of these artifacts could be corrected using a spherical solvent boundary potential and extended electrostatics with no cutoff.[47] An interesting and alternative solution was also developed by Åqvist et al.[48] where the partial charges of the coordinating carbonyl atoms were increased to reflect the polarization effects of the protein. With our multisite ion model, we observe no problems with coordination geometries or secondary structure, we are still able to use techniques such as Particle Mesh Ewald[49] for long-range electrostatics, and we do not need to alter the atomic charges of the protein.

In order to test thermodynamic predictions using our ion model, we looked at the selectivity of Site II for Ca^{2+} over Mg^{2+}. Experimentally, the binding free energy difference for these two ions is $\Delta\Delta G = 4.9 \pm 0.14$ kcal/mol with calcium having a higher affinity.[28] In separate simulations using both a spherical ion and our multisite ion, we started with the calcium bound structure and performed thermodynamic integration where the

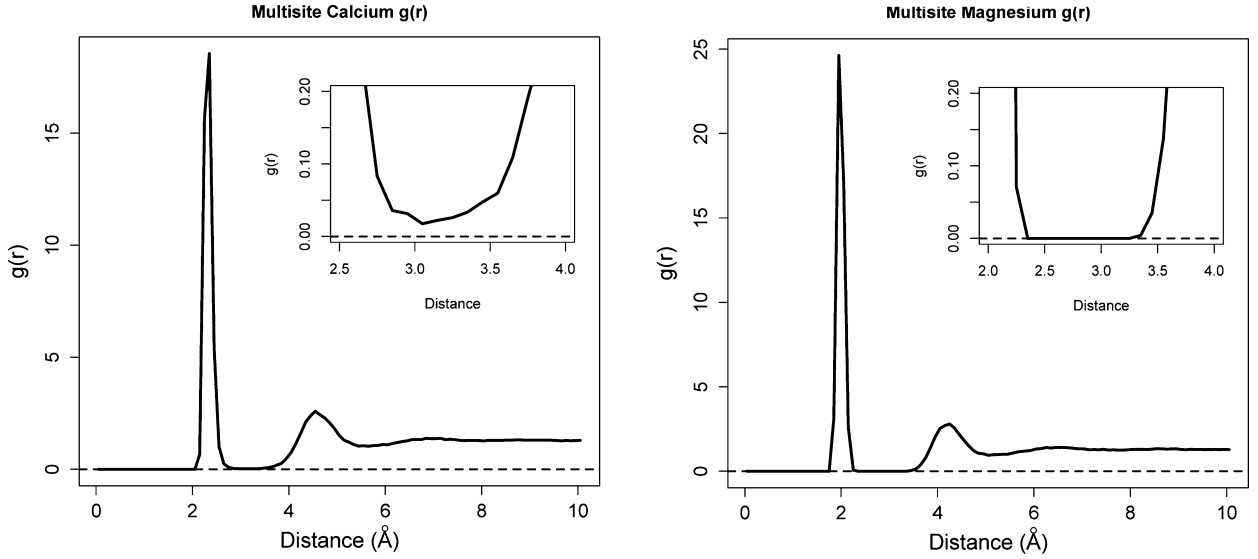

Figure 2. Radial distribution functions for our calcium and magnesium models. The nonzero g(r) value between the two solvation shells of calcium is consistent with the solvent exchange we observe.

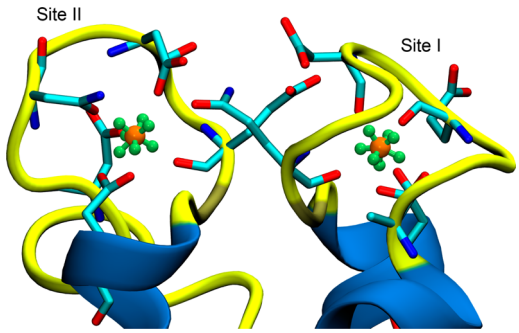

Figure 3. EF hand motifs of calbindin with our multisite ion in both Site I and Site II.

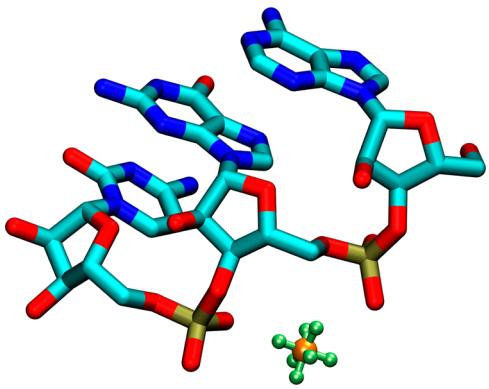

Figure 4. Bidentate clamp structure with out multisite ion coordinated by two adjacent RNA bases.

calcium was slowly changed to magnesium. To simulate the reverse transition, we started with the Mg^{2+}-calbindin structure and slowly changed the bound magnesium into calcium. This structure differs slightly from the calcium structure; the biggest difference being the presence of a coordinating water molecule. The predicted free energy difference using our multisite model was $\Delta\Delta G = 4.5 \pm 1.2$ kcal/mol, in agreement with experiment, while the spherical ion gave a much larger value of $\Delta\Delta G = 12.7 \pm 1.6$ kcal/mol. Having promising results for the ion-protein case, we moved on the much more challenging problem of divalent cations and nucleic acids.

The issues surrounding the use of divalent cations in molecular simulations of nucleic acids are well-known in the field but rather poorly documented.[50,51] These ions, particularly magnesium, play special roles in the folding and interaction of both RNA and DNA, but the charge density of the phosphate backbone causes significant problems in predicting both geometries and thermodynamic quantities. As a model of the relatively simple RNA–Mg^{2+} complex, we selected a bidentate clamp where magnesium is tightly coordinated by the phosphate of two neighboring bases (see Figure 4). This is a common motif in crystal structures, and just as with the EF hand, this motif is highly selective, but in this case, favors Mg^{2+} over Ca^{2+}. Petrov et al.[29] completed a series of quantum calculations and found a binding energy difference of $\Delta\Delta E = -10.4$ kcal/mol, favoring the RNA^{2-}–Mg^{2+} complex. Our multisite model predicts a difference in affinity of $\Delta\Delta G = -18.4 \pm 0.6$ kcal/mol while the spherical ion model fails completely, giving a prediction of $\Delta\Delta G = +12.6 \pm 0.6$ kcal/mol indicating more favorable binding of calcium. The discrepancy between our multisite model and the quantum calculations is somewhat larger than we found in the protein case; however, the quantum calculation does not include entropy differences, which considering the solvation differences should shift the quantum $\Delta\Delta E$ value in the negative direction, closer to our value.

CONCLUDING REMARKS

Taken together, our multisite cation model presents a number of advantages over standard, spherical ion models. The solvation, binding thermodynamics, and coordination geometries are all improved using this model. Further, this model is compatible with standard molecular force fields and requires negligible additional computational cost.

ASSOCIATED CONTENT

Supporting Information

Simulation parameter files. This material is available free of charge via the Internet at http://pubs.acs.org.

AUTHOR INFORMATION

Corresponding Author

*Phone: (734) 615-9587. E-mail: dsept@umich.edu.

Author Contributions

The manuscript was written through contributions of both authors, and both have given approval to the final version of the manuscript.

Notes

The authors declare no competing financial interest.

REFERENCES

(1) Jensen, K. P.; Jorgensen, W. L. *J. Chem. Theory Comput.* **2006**, *2*, 1499.
(2) Aqvist, J. *J. Phys. Chem.* **1990**, *94*, 8021.
(3) Joung, I. S.; Cheatham, T. E. *J. Phys. Chem. B* **2008**, *112*, 9020.
(4) Alejandre, J.; Hansen, J. P. *Phys. Rev. E* **2007**, 76.
(5) Beglov, D.; Roux, B. *J. Chem. Phys.* **1994**, *100*, 9050.
(6) Dang, L. X. *J. Am. Chem. Soc.* **1995**, *117*, 6954.
(7) Straatsma, T. P.; Berendsen, H. J. C. *J. Chem. Phys.* **1988**, *89*, 5876.
(8) Teleman, O.; Ahlstrom, P. *J. Am. Chem. Soc.* **1986**, *108*, 4333.
(9) Weerasinghe, S.; Smith, P. E. *J. Chem. Phys.* **2003**, *119*, 11342.
(10) Whitfield, T. W.; Varma, S.; Harder, E.; Lamoureux, G.; Rempe, S. B.; Roux, B. *J. Chem. Theory Comput.* **2007**, *3*, 2068.
(11) Grossfield, A.; Ren, P. Y.; Ponder, J. W. *J. Am. Chem. Soc.* **2003**, *125*, 15671.
(12) Lamoureux, G.; Roux, B. *J. Phys. Chem. B* **2006**, *110*, 3308.
(13) Piquemal, J. P.; Perera, L.; Cisneros, G. A.; Ren, P. Y.; Pedersen, L. G.; Darden, T. A. *J. Chem. Phys.* **2006**, *125*, 054511.
(14) Yu, H. B.; Whitfield, T. W.; Harder, E.; Lamoureux, G.; Vorobyov, I.; Anisimov, V. M.; MacKerell, A. D.; Roux, B. *J. Chem. Theory Comput.* **2010**, *6*, 774.
(15) Aqvist, J.; Warshel, A. *J. Am. Chem. Soc.* **1990**, *112*, 2860.
(16) Aqvist, J.; Warshel, A. *J. Mol. Biol.* **1992**, *224*, 7.
(17) Pang, Y. P. *J. Mol. Model.* **1999**, *5*, 196.
(18) Pang, Y. P.; Xu, K.; El Yazal, J.; Prendergast, F. G. *Protein Sci.* **2000**, *9*, 1857.
(19) Oelschlaeger, P.; Klahn, M.; Beard, W. A.; Wilson, S. H.; Warshel, A. *J. Mol. Biol.* **2007**, *366*, 687.
(20) Pauling, L. *J. Am. Chem. Soc.* **1929**, *51*, 1010.
(21) Strynadka, N. C. J.; James, M. N. G. *Annu. Rev. Biochem.* **1989**, *58*, 951.
(22) Falke, J. J.; Drake, S. K.; Hazard, A. L.; Peersen, O. B. *Q. Rev. Biophys.* **1994**, *27*, 219.
(23) Frisch, M. J.; Trucks, G. W.; Schlegel, H. B.; Scuseria, G. E.; Rob, M. A.; Cheeseman, J. R.; Montgomery, J. A.; Vreven, T.; Kudin, K. N.; Burant, J. C.; Millam, J. M. *GAUSSIAN*; Gaussian, Inc.: Wallingford, CT, 2003.
(24) Katz, A. K.; Glusker, J. P.; Beebe, S. A.; Bock, C. W. *J. Am. Chem. Soc.* **1996**, *118*, 5752.
(25) Markham, G. D.; Glusker, J. P.; Bock, C. W. *J. Phys. Chem. B* **2002**, *106*, 5118.
(26) Case, D. A.; Darden, T. A.; T.E. Cheatham, I.; Simmerling, C. L.; Wang, J.; Duke, R. E.; Luo, R.; Walker, R. C.; Zhang, W.; Merz, K. M.; Roberts, B.; Wang, B.; Hayik, S.; Roitberg, A.; Seabra, G.; Kolossvary, I.; Wong, K. F.; Paesani, F.; Vanicek, J.; Liu, J.; Wu, X.; Brozell, S. R.; Steinbrecher, T.; Gohlke, H.; Cai, Q.; Ye, X.; Wang, J.; Hsieh, M.-J.; Cui, G.; Roe, D. R.; Matthews, D. H.; Seetin, M. G.; Sagui, C.; Babin, V.; Luchko, T.; Gusarov, S.; Kovalenko, A.; Kollman, P. A. *AMBER*; University of California: San Francisco, 2010.
(27) Szebenyi, D. M. E.; Moffat, K. *J. Biol. Chem.* **1986**, *261*, 8761.
(28) Andersson, M.; Malmendal, A.; Linse, S.; Ivarsson, I.; Forsen, S.; Svensson, L. A. *Protein Sci.* **1997**, *6*, 1139.
(29) Petrov, A. S.; Bowman, J. C.; Harvey, S. C.; Williams, L. D. *RNA* **2011**, *17*, 291.
(30) Ferre-D'Amare, A. R.; Zhou, K. H.; Doudna, J. A. *Nature* **1998**, *395*, 567.
(31) Perez, A.; Marchan, I.; Svozil, D.; Sponer, J.; Cheatham, T. E.; Laughton, C. A.; Orozco, M. *Biophys. J.* **2007**, *92*, 3817.
(32) Noyes, R. M. *J. Am. Chem. Soc.* **1962**, *84*, 513.
(33) Hunenberger, P. H.; McCammon, J. A. *Biophys. Chem.* **1999**, *78*, 69.
(34) Neely, J.; Connick, R. *J. Am. Chem. Soc.* **1970**, *92*, 3476.
(35) Bleuzen, A.; Pittet, P. A.; Helm, L.; Merbach, A. E. *Magn. Reson. Chem.* **1997**, *35*, 765.
(36) Helm, L.; Merbach, A. E. *Coordin. Chem. Rev.* **1999**, *187*, 151.
(37) Ohtaki, H.; Radnai, T. *Chem. Rev.* **1993**, *93*, 1157.
(38) Badyal, Y. S.; Barnes, A. C.; Cuello, G. J.; Simonson, J. M. *J. Phys. Chem. A* **2004**, *108*, 11819.
(39) Jalilehvand, F.; Spangberg, D.; Lindqvist-Reis, P.; Hermansson, K.; Persson, I.; Sandstrom, M. *J. Am. Chem. Soc.* **2001**, *123*, 431.
(40) Marcus, Y. *Chem. Rev.* **1988**, *88*, 1475.
(41) Schwenk, C. F.; Rode, B. M. *Pure Appl. Chem.* **2004**, *76*, 37.
(42) Larentzos, J. P.; Criscenti, L. J. *J. Phys. Chem. B* **2008**, *112*, 14243.
(43) Naor, M. M.; Van Nostrand, K.; Dellago, C. *Chem. Phys. Lett.* **2003**, *369*, 159.
(44) Owczarek, E.; Rybicki, M.; Hawlicka, E. *J Phys Chem B* **2007**, *111*, 14271.
(45) Ahlstrom, P.; Teleman, O.; Kordel, J.; Forsen, S.; Jonsson, B. *Biochemistry* **1989**, *28*, 3205.
(46) Kordel, J.; Teleman, O. *J. Am. Chem. Soc.* **1992**, *114*, 4934.
(47) Marchand, S.; Roux, B. *Proteins* **1998**, *33*, 265.
(48) Aqvist, J.; Alvarez, O.; Eisenman, G. *Jerus Sym Q* **1992**, *25*, 367.
(49) Darden, T.; York, D.; Pedersen, L. *J. Chem. Phys.* **1993**, *98*, 10089.
(50) Cheatham, T. E.; Young, M. A. *Biopolymers* **2001**, *56*, 232.
(51) Perez, A.; Luque, F. J.; Orozco, M. *Acc. Chem. Res.* **2012**, *45*, 196.